ACS Catalysis

Letter

pubs.acs.org/acscatalysis

Functionalized Ruthenium–Phosphine Metal–Organic Framework for Continuous Vapor-Phase Dehydrogenation of Formic Acid

Amaia Beloqui Redondo,[†,‡] Flavien L. Morel,[†,‡] Marco Ranocchiari,[*,§] and Jeroen A. van Bokhoven[*,†,§]

[†]Institute for Chemical and Bioengineering, ETH Zürich, Vladimir-Prelog-Weg 1, CH-8093 Zürich, Switzerland

[§]Laboratory for Catalysis and Sustainable Chemistry, Paul Scherrer Institute, CH-5232 Villigen, Switzerland

Supporting Information

ABSTRACT: Metal–organic frameworks (MOFs) are ideal hosts for incorporation of molecular complexes without altering their original ligand environment; molecular catalysts can thus be easily synthesized and used in gas- and vapor-phase reactions operated in continuous mode. We report the immobilization of a molecular ruthenium complex in a phosphine-functionalized MOF that is highly efficient in the vapor-phase dehydrogenation of formic acid. The catalyst exhibited exclusive selectivity to hydrogen and carbon dioxide with outstanding stability at 145 °C (TON > 1 290 000). Our results represent a noteworthy improvement over heterogeneous ruthenium systems in terms of selectivity in the gas-phase, while reaching a productivity level higher than that of state-of-the-art homogeneous catalysts.

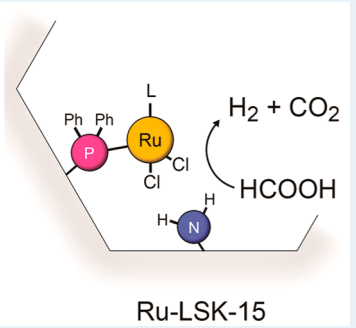

KEYWORDS: *formic acid, heterogeneous catalyst, metal–organic framework, phosphine, ruthenium*

MOFs are emerging as valuable materials for a wide range of applications such as gas storage[1,2] and separation,[3,4] sensing applications,[5] and drug delivery.[6,7] MOFs demonstrate enormous potential as heterogeneous catalysts[8−15] in light of their considerable structural and chemical versatility,[16−18] including for the liquid-phase decomposition of formic acid.[19,20] Their advantages over molecular and supported catalysts are gradually becoming evident. Molecular catalysts are primarily associated with homogeneous complexes applied in the liquid phase. Their use in the gas or vapor phase is rather limited because of their lack of active surface. However, efforts have been made to immobilize molecular complexes on solid supports to make them suitable for gas-phase reactions and facilitate their recovery.[21,22] MOFs provide a unique opportunity to host molecular catalysts within a cavity of controlled size and apply them in gas-phase reactions. The tunability of functional groups in a MOF enables heterogenization of molecular catalysts without altering their ligand coordination sphere.[23,24] MOFs with phosphine functional groups can fulfill organocatalytic[25] and solid support roles, where the phosphine provides an anchoring point for metal coordination. They represent a relatively simple but elegant vessel for incorporation of catalytic active centers with atomic precision into a solid structure.[24,26,27]

Research focused on using hydrogen as energy feedstock represents an important field due to the growing demand in alternative energy technologies.[28−30] Decomposition of formic acid can proceed via dehydrogenation to form hydrogen and carbon dioxide or via dehydration, producing water and carbon monoxide. Processes that favor the exclusive formation of hydrogen have to be developed. Liquid-phase formic acid decomposition has been performed at ambient temperature with palladium nanoparticles embedded within MIL-125, achieving a turnover frequency (TOF) of 214 h^{-1}.[20] A similar system was prepared with Au–Pd nanoparticles immobilized in MIL-101.[19] These systems are outperformed by homogeneous catalysts in term of activity, selectivity, and stability.[31,32] In recent years, notable advances in the design of homogeneous catalysts for formic acid decomposition have been made by the groups of Beller and Laurenczy with ruthenium and rhodium complexes used in conjunction with amine additives.[32−37] Despite the considerable number and variety of ruthenium catalysts used for this reaction, few heterogeneous ruthenium catalysts have been developed.[38−40]

Our group recently described the preparation method of a bifunctional MOF called LSK-15 that exhibits the MIL-101(Al) topology (Figure 1a) and which contains phosphino and amino functional groups to form $[Al_3O(Cl,OH)(NH_2–C_8H_3O_4)_{2.64}(PPh_2\text{-}C_8H_3O_4)_{0.36}]_n$.[41,42] LSK-15 is an ideal material for formic acid decomposition because (a) the MIL-101 topology shows good chemical and thermal stability and its large pores and cages can easily accommodate transition-metal complexes and substrates for reaction,[23,43,44] (b) phosphine moieties are strong anchoring sites for transition-metal complexes, and (c) amine moieties provide a local basic environment that is thought to facilitate the activation of formic acid, in a manner reminiscent of homogeneous systems.[37] Here we report a very stable and selective MOF catalyst for the vapor-phase dehydrogenation of formic acid. To illustrate the

Received: September 8, 2015
Revised: October 28, 2015
Published: November 2, 2015

DOI: 10.1021/acscatal.5b01987
ACS Catal. 2015, 5, 7099−7103

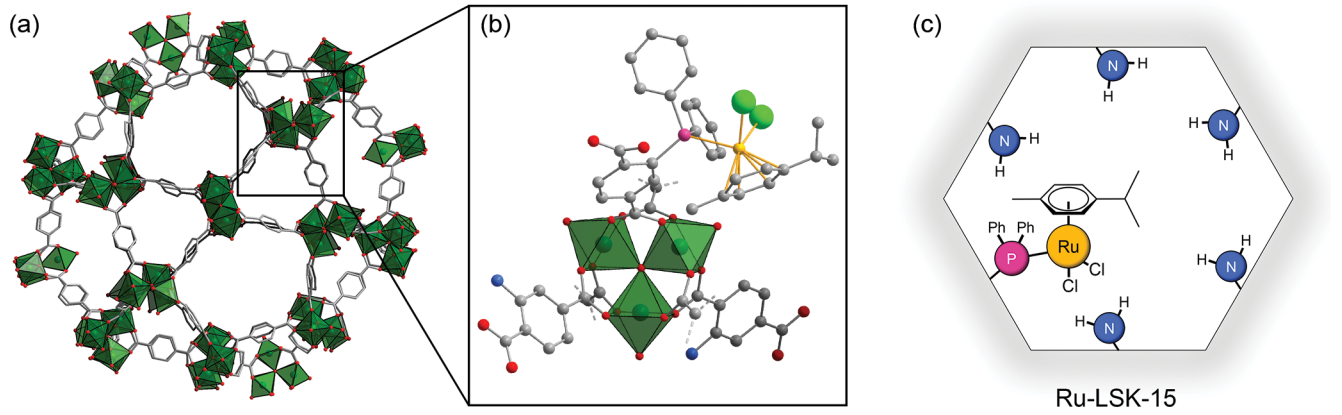

Figure 1. (a) General representation of the MIL-101 pore system (green = aluminum, red = oxygen, gray = carbon). (b) Molecular representation of the local environment in Ru-LSK-15 with phosphine and amine linkers (pink = phosphorus, blue = nitrogen, orange = ruthenium, light green = chloride). Hydrogen atoms are omitted for clarity. (c) Schematic representation of the ruthenium, phosphine, and amine functionalities present in the MOF cages.

suitability of molecular complexes in phosphine-MOFs for gas-phase reactions, and inspired by the activity of ruthenium molecular catalysts in liquid-phase formic acid decomposition, we introduced ruthenium into LSK-15 by postsynthetic modification to form [Ru(*p*-cym) (PPh_2-MOF)Cl_2] (Ru-LSK-15). We synthesized the orange solid Ru-LSK-15 (Figure 1b,c) by reacting $[Ru(p\text{-cym})Cl_2]_2$ with LSK-15 in dichloromethane for 24 h, adapting existing procedures for related organometallic complexes.[45,46]

The material retained its crystalline structure upon coordination and showed a decrease in pore volume from 1.26 to 0.6 cm^3/g (Figure S1–S2, Supporting Information). This space-filling effect was already described in a similar system[23] and is attributed to the ruthenium complex inside the cage of LSK-15. The ^{31}P NMR spectrum of the impregnated material (Figure S3, Supporting Information) showed two additional features at +19 ppm and +33 ppm not present in LSK-15. These are in the region of phosphine–ruthenium coordination and phosphine oxide species.[45]

The ^{13}C NMR spectrum displayed features from the coordinated *para*-cymene from +17 to +35 ppm, thus confirming the presence of the ruthenium sites in a chemical environment analogous to [Ru(*p*-cym) (PPh_3)Cl_2].[45,46] Partial coordination of the phosphine groups is in agreement with a ruthenium loading of 0.4 ± 0.2 wt %, as measured by atomic absorption spectroscopy (Table S1, Supporting Information). A low ruthenium loading presents the advantages of enhanced diffusivity within the pore system and maximizes the access to the catalytic sites.

Dehydrogenation of formic acid was carried out in a fixed bed at different temperatures (125, 145, and 165 °C) to investigate the catalytic performance of Ru-LSK-15 in the vapor-phase. Figure 2a,b shows the formic acid conversion (a) and selectivities to hydrogen and carbon monoxide (b) as the reactor temperature was switched between 125, 145, and 165 °C in 24 h allotments. During the first 24 h at 125 °C an induction period was observed in which the conversion of formic acid increased from 7 to 34 ± 13%. The conversion stabilized at 75 ± 5% (TOF = 2000 ± 440 h^{-1}) once the temperature was increased to 145 °C. Conversion increased further to 88 ± 8% (TOF = 2400 ± 580 h^{-1}) after reaching 165 °C and remained constant for 24 h. No sign of deactivation was observed within this period, and an overall turnover number

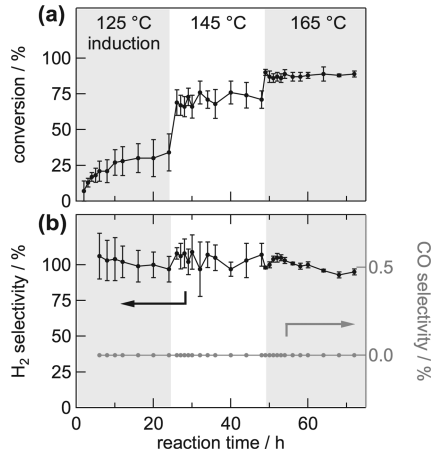

Figure 2. (a) Formic acid conversion and (b) selectivity to hydrogen and carbon monoxide with time while switching the reaction temperature between 125, 145, and 165 °C. Error bars represent the standard deviation of four consecutive measurements.

(TON) of 121 300 was calculated. The hydrogen selectivity was recorded above 99% for the major part of the experiment, with a decrease to 97 ± 2% in the last few hours. Neither residual dichloromethane nor carbon monoxide was detected, but trace methanol was found by gas chromatography. Conversion values with large standard deviations were observed over the first 24 h prior to the system attaining steady-state conditions. As the reactor was heated to 145 and 165 °C, the system evolved hydrogen and carbon dioxide at a constant rate. A similar activation was observed when ramping the reactor temperature up and then down, giving higher conversion values at the same temperature on the downward ramp (Figure S4a, Supporting Information). We attribute the observed induction period to a mechanism involving the elimination of chloride ligands from the metal complex before the coordination of formates, following the proposal made by Morris et al. for the generation of hydrogen from formic acid by ruthenium complexes.[47] Amines have been reported to act as proton scavengers in the liquid phase by deprotonating formic acid to create formate.[40] It is possible that the amine moieties on LSK-15 fulfill a similar role in the decomposition mechanism as we observed their protonation after catalytic testing (vide infra).

DOI: 10.1021/acscatal.5b01987
ACS Catal. 2015, 5, 7099–7103

To investigate the coordinating role of the phosphine groups in LSK-15, we performed the reaction in the presence of ruthenium with MIL-101(Al)-NH_2 as support. Using the same postsynthetic impregnation procedure as for Ru-LSK-15 resulted in considerable leaching during the washing step, suggesting weak ruthenium−amine coordination. Instead, we prepared Ru@MIL-101(Al)-NH_2 by incipient-wetness impregnation of MIL-101(Al)-NH_2 with a $[Ru(p\text{-cym})Cl_2]_2$ solution containing a similar amount of ruthenium as in Ru-LSK-15 (see Supporting Information). With this material, a maximum formic acid conversion of only 11 ± 3% at 165 °C (TOF = 308 ± 130 h^{-1}) was obtained (Figure S4b, Supporting Information). These observations indicate that phosphine groups are essential for anchoring the ruthenium complex and establishing a defined and highly efficient active site. This behavior is easily explained by the stronger ability of phosphines to coordinate ruthenium, as compared to monodentate amines. No conversion was detected for LSK-15 in the absence of ruthenium complex at an operational temperature of 165 °C, thereby ruling out any intrinsic activity of the framework and autodecomposition of the substrate.

Heterogeneous catalysts in the vapor-phase decomposition of formic acid suffer from lower selectivity and activity than molecular counterparts, commonly used in the liquid-phase reaction.[38,40,48] By immobilizing a molecular catalyst within a phosphine-MOF, we transfer its catalytic performance to gas-phase applications. Our ruthenium catalyst showed high stability with no detectable carbon monoxide formation under the conditions described. A long-term experiment was conducted to verify the stability of Ru-LSK-15 (ramp to 125 °C and 24 h dwell time before ramping to 145 °C, Figure 3a). The vapor-phase formic acid decomposition was performed for 23 days at 145 °C. Under these conditions, Ru-LSK-15 gave a constant TOF of 2300 ± 570 h^{-1}. A TON of 1 290 000 was reached without measurable deactivation, suggesting that the catalyst may continue to operate for an even longer period of time. Transmission electron microscopy (TEM) performed on this sample after catalysis showed no ruthenium particle formation after 23 days (Figure 3b). The micrograph looks essentially identical to the as-prepared material. Micrographs of samples before and after all experiments are shown in the Supporting Information (Figure S5). Energy-dispersive X-ray (EDX) spectroscopy confirmed the presence of ruthenium in the observed field of view (Figure S6, Supporting Information). Although electron micrographs can be difficult to assess due to the interaction between the sample and the electron beam,[49] we do observe the conservation of the molecular structure as characterized by the absence of large ruthenium clusters. This is a remarkable result considering the relatively harsh conditions of the reaction. We attribute the robustness of the catalyst to the coordination strength of phosphine groups within the material, which prevents sintering.

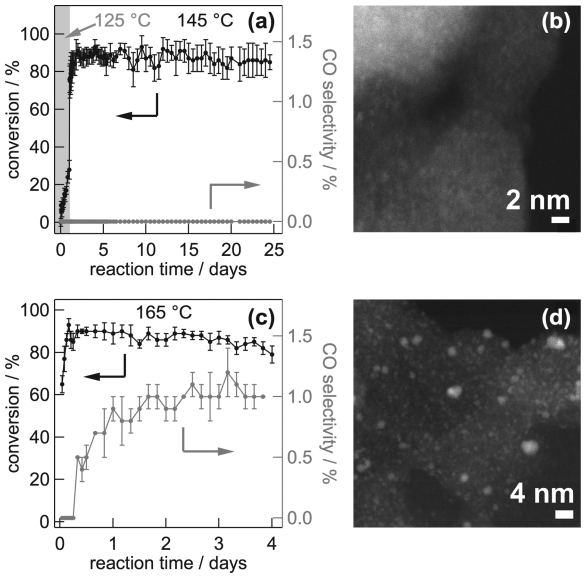

Figure 3. Formic acid conversion (black, left axis), carbon monoxide selectivity (gray, right axis) with time. HAADF-STEM images after reaction of Ru-LSK-15 at 145 °C (a,b) and at 165 °C after fast activation (c,d). Error bars represent the standard deviation of four consecutive measurements.

In terms of stability, Ru-LSK-15 matches the highest reported TON values for the dehydrogenation of formic acid, both in liquid and gas-phase. In comparison with supported ruthenium nanoparticles in the gas-phase,[38,40] Ru-LSK-15 showed a large improvement in terms of activity and selectivity. This highlights the advantages of immobilized complexes that couple the high efficiency of homogeneous systems[50] and the convenience of heterogeneous catalysts, as well as expanding their application to operation in the gas phase and thus to easy operation in continuous mode. A more comprehensive comparison of performance in the dehydrogenation of formic acid between our catalyst and selected heterogeneous and homogeneous catalysts reported in the literature can be found in the Supporting Information (Table S2). Additionally, a catalytic run under harsher reaction conditions, using a faster heating ramp to 165 °C and higher flow of formic acid, for 4 days gave an initial TOF of 4200 ± 800 h^{-1} after a short induction period (Figure 3c). Carbon monoxide was observed after 8 h, reaching a selectivity of 1.0 ± 0.2% after 2 days. TEM micrographs of the sample after reaction confirmed the formation of ruthenium clusters and particles (Figure 3d), indicating that the molecularly dispersed metal centers are essential for reaching high selectivity.

A comparison of the X-ray diffraction powder patterns of the catalyst before and after the reaction (Figure S7c,d, Supporting Information) indicates a partial loss of the long-range order of the MOF. Nitrogen physisorption data (Figure S7e,f, Supporting Information) reveal a considerable decrease in BET surface area and total pore volume after reaction from 1075 to 161 m^2/g and 0.61 to 0.19 cm^3/g, respectively. These values are consistent with the long-range loss in order observed by X-ray diffraction. XRD patterns measured during the induction period after 12 h at 125 °C indicated that the loss in long-range order occurred gradually (Figure S8, Supporting Information). The high activity displayed by the catalyst, despite a partial collapse of the framework, suggests that the short-range order is the crucial parameter to maintain the integrity of molecular catalysts. ^{31}P solid-state MAS NMR spectrum of the material recovered after catalysis showed a substantial decrease of signals related to free phosphine (Figure 4, left). Samples of LSK-15 exposed to air or formic acid (Figure S9, Supporting Information) reveal that signals between +30 and +40 ppm are likely to originate from a mixture of phosphine oxide and the ruthenium−phosphine complex. ^{13}C NMR spectra (Figure 4, right) depict clear signals arising from the organic linkers and ligands. Carbon signals attributed to the amino linker[51] at +150 ppm and +116 ppm

DOI: 10.1021/acscatal.5b01987
ACS Catal. 2015, 5, 7099−7103

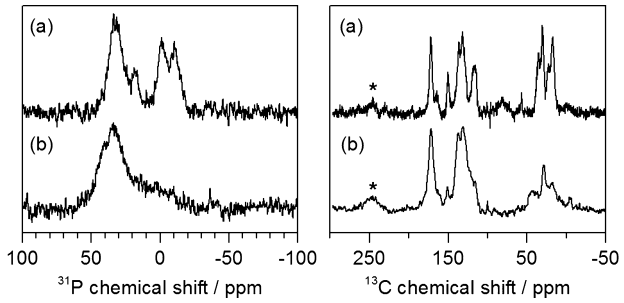

Figure 4. ^{31}P (left) and ^{13}C (right) MAS NMR spectra of Ru-LSK-15 before (a) and after reaction (b). Spinning sidebands are marked with (*).

declined markedly in intensity after the reaction. These observations are in agreement with the chemical shifts of the protonated linker, which coalesce in the +130 ppm region. This highlights a possible future improvement of the material, in which the basic environment of LSK-15 could be further tuned to increase its reactivity toward the deprotonation of the formic acid. A carbon signal at +172 ppm shows that the carboxylate bond responsible for the short-range order within the framework is preserved and is further confirmed by the exclusive presence of octahedral aluminum, as observed in the ^{27}Al NMR spectra (Figure S10, Supporting Information).

In summary, we designed and prepared a multifunctional MOF catalyst containing a single-site molecular ruthenium complex of the form [$RuCl_2$(*p*-cym) (PPh_2-MOF)] and determined its excellent performance in the vapor-phase dehydrogenation of formic acid. Phosphine moieties drive the formation of ruthenium single-sites inside a heterogeneous support. In addition, they ensure preservation of the original ligand coordination sphere and thus of the catalytically active site. The resulting material displayed high selectivity for hydrogen and a TON larger than 1 290 000 in the dehydrogenation of formic acid. We demonstrate that MOFs with multiple functional groups are compelling candidates for establishing single-site heterogeneous catalysts for vapor-phase reaction operated in continuous mode.

■ ASSOCIATED CONTENT

Supporting Information

The Supporting Information is available free of charge on the ACS Publications website at DOI: 10.1021/acscatal.5b01987.

Synthesis of Ru-LSK-15 and Ru@MIL-101(Al)-NH_2; additional catalytic experiments; X-ray diffraction patterns; nitrogen physisorption isotherms; TEM and EDX pictures; MAS NMR spectra; catalytic performance of selected literature examples (PDF)

■ AUTHOR INFORMATION

Corresponding Authors

*E-mail: marco.ranocchiari@psi.ch.

*E-mail: j.a.vanbokhoven@chem.ethz.ch.

Author Contributions

‡A.B.R and F.L.M contributed equally.

Notes

The authors declare no competing financial interest.

■ ACKNOWLEDGMENTS

The authors thank Malwina Staniuk (low-angle XRD), Dr. Frank Krumeich (TEM), and Dr. Kim Meyer (MIL-101(Al)-NH_2 synthesis). This research was supported by ETH Zurich (ETHIIRA proposal ETH-33 11-1).

■ REFERENCES

(1) Makal, T. A.; Li, J.-R.; Lu, W.; Zhou, H.-C. *Chem. Soc. Rev.* **2012**, *41*, 7761−7779.
(2) Farha, O. K.; Eryazici, I.; Jeong, N. C.; Hauser, B. G.; Wilmer, C. E.; Sarjeant, A. A.; Snurr, R. Q.; Nguyen, S. T.; Yazaydin, A. Ö.; Hupp, J. T. *J. Am. Chem. Soc.* **2012**, *134*, 15016−15021.
(3) Li, J.-R.; Kuppler, R. J.; Zhou, H.-C. *Chem. Soc. Rev.* **2009**, *38*, 1477−1504.
(4) Rodenas, T.; Luz, I.; Prieto, G.; Seoane, B.; Miro, H.; Corma, A.; Kapteijn, F.; Llabrés i Xamena, F. X.; Gascon, J. *Nat. Mater.* **2015**, *14*, 48−55.
(5) Shekhah, O.; Liu, J.; Fischer, R. A.; Wöll, C. *Chem. Soc. Rev.* **2011**, *40*, 1081−1106.
(6) Horcajada, P.; Gref, R.; Baati, T.; Allan, P. K.; Maurin, G.; Couvreur, P.; Férey, G.; Morris, R. E.; Serre, C. *Chem. Rev.* **2012**, *112*, 1232−1268.
(7) Keskin, S.; Kızılel, S. *Ind. Eng. Chem. Res.* **2011**, *50*, 1799−1812.
(8) Gascon, J.; Corma, A.; Kapteijn, F.; Llabrés i Xamena, F. X. *ACS Catal.* **2014**, *4*, 361−378.
(9) Farrusseng, D.; Aguado, S.; Pinel, C. *Angew. Chem., Int. Ed.* **2009**, *48*, 7502−7513.
(10) Ranocchiari, M.; van Bokhoven, J. A. *Phys. Chem. Chem. Phys.* **2011**, *13*, 6388−6396.
(11) Liu, J.; Chen, L.; Cui, H.; Zhang, J.; Zhang, L.; Su, C.-Y. *Chem. Soc. Rev.* **2014**, *43*, 6011−6061.
(12) Bing, L.; Suyun, J.; Bogen, L. *Prog. Chem.* **2013**, *1*, 36−45.
(13) Isaeva, V. I.; Kustov, L. M. *Pet. Chem.* **2010**, *50*, 167−180.
(14) Santos, V. P.; Wezendonk, T. A.; Jaén, J. J. D.; Dugulan, A. I.; Nasalevich, M. A.; Islam, H.-U.; Chojecki, A.; Sartipi, S.; Sun, X.; Hakeem, A. A.; Koeken, A. C. J.; Ruitenbeek, M.; Davidian, T.; Meima, G. R.; Sankar, G.; Kapteijn, F.; Makkee, M.; Gascon, J. *Nat. Commun.* **2015**, *6*, 6451.
(15) Ranocchiari, M.; Lothschütz, C.; Grolimund, D.; van Bokhoven, J. A. *Proc. R. Soc. London, Ser. A* **2012**, *468*, 1985−1999.
(16) Evans, J. D.; Sumby, C. J.; Doonan, C. J. *Chem. Soc. Rev.* **2014**, *43*, 5933−5951.
(17) Deria, P.; Mondloch, J. E.; Karagiaridi, O.; Bury, W.; Hupp, J. T.; Farha, O. K. *Chem. Soc. Rev.* **2014**, *43*, 5896−5912.
(18) Cohen, S. M. *Chem. Rev.* **2012**, *112*, 970−1000.
(19) Gu, X.; Lu, Z.; Jiang, H.; Akita, T.; Xu, Q. *J. Am. Chem. Soc.* **2011**, *133*, 11822−11825.
(20) Martis, M.; Mori, K.; Fujiwara, K.; Ahn, W.; Yamashita, H. *J. Phys. Chem. C* **2013**, *117*, 22805−22810.
(21) Copéret, C.; Chabanas, M.; Petroff Saint-Arroman, R.; Basset, J.-M. *Angew. Chem., Int. Ed.* **2003**, *42*, 156−181.
(22) Fraile, J. M.; García, J. I.; Mayoral, J. A. *Chem. Rev.* **2009**, *109*, 360−417.
(23) Canivet, J.; Aguado, S.; Schuurman, Y.; Farrusseng, D. *J. Am. Chem. Soc.* **2013**, *135*, 4195−4198.
(24) Falkowski, J. M.; Sawano, T.; Zhang, T.; Tsun, G.; Chen, Y.; Lockard, J. V.; Lin, W. *J. Am. Chem. Soc.* **2014**, *136*, 5213−5216.
(25) Xu, X.; van Bokhoven, J. A.; Ranocchiari, M. *ChemCatChem* **2014**, *6*, 1887−1891.
(26) Fritsch, J.; Drache, F.; Nickerl, G.; Böhlmann, W.; Kaskel, S. *Microporous Mesoporous Mater.* **2013**, *172*, 167−173.
(27) Václavík, J.; Servalli, M.; Lothschütz, C.; Szlachetko, J.; Ranocchiari, M.; van Bokhoven, J. A. *ChemCatChem* **2013**, *5*, 692−696.
(28) Crabtree, G. W.; Dresselhaus, M. S.; Buchanan, M. V. *Phys. Today* **2004**, *57*, 39−44.
(29) Joó, F. *ChemSusChem* **2008**, *1*, 805−808.
(30) Dunn, S. *Int. J. Hydrogen Energy* **2002**, *27*, 235−264.

DOI: 10.1021/acscatal.5b01987
ACS Catal. 2015, 5, 7099−7103

(31) Jezequel, M.; Dufaud, V.; Ruiz-Garcia, M. J.; Carrillo-Hermosilla, F.; Neugebauer, U.; Niccolai, G. P.; Lefebvre, F.; Bayard, F.; Corker, J.; Fiddy, S.; Evans, J.; Broyer, J. P.; Malinge, J.; Basset, J. M. *J. Am. Chem. Soc.* **2001**, *123*, 3520−3540.
(32) Boddien, A.; Mellmann, D.; Gärtner, F.; Jackstell, R.; Junge, H.; Dyson, P. J.; Laurenczy, G.; Ludwig, R.; Beller, M. *Science* **2011**, *333*, 1733−1736.
(33) Loges, B.; Boddien, A.; Junge, H.; Beller, M. *Angew. Chem., Int. Ed.* **2008**, *47*, 3962−3965.
(34) Fellay, C.; Dyson, P. J.; Laurenczy, G. *Angew. Chem., Int. Ed.* **2008**, *47*, 3966−3968.
(35) Boddien, A.; Gärtner, F.; Mellmann, D.; Sponholz, P.; Junge, H.; Laurenczy, G.; Beller, M. *Chimia* **2011**, *65*, 214−218.
(36) Thevenon, A.; Frost-Pennington, E.; Weijia, G.; Dalebrook, A. F.; Laurenczy, G. *ChemCatChem* **2014**, *6*, 3146−3152.
(37) Junge, H.; Boddien, A.; Capitta, F.; Loges, B.; Noyes, J. R.; Gladiali, S.; Beller, M. *Tetrahedron Lett.* **2009**, *50*, 1603−1606.
(38) Solymosi, F.; Koós, Á.; Liliom, N.; Ugrai, I. *J. Catal.* **2011**, *279*, 213−219.
(39) Gan, W.; Dyson, P. J.; Laurenczy, G. *ChemCatChem* **2013**, *5*, 3124−3130.
(40) Zacharska, M.; Podyacheva, O. Y.; Kibis, L. S.; Boronin, A. I.; Senkovskiy, B. V.; Gerasimov, E. Y.; Taran, O. P.; Ayusheev, A. B.; Parmon, V. N.; Leahy, J. J.; Bulushev, D. A. *ChemCatChem* **2015**, *7*, 2910−2917.
(41) Morel, F. L.; Ranocchiari, M.; van Bokhoven, J. A. *Ind. Eng. Chem. Res.* **2014**, *53*, 9120−9127.
(42) Morel, F. L.; Pin, S.; Huthwelker, T.; Ranocchiari, M.; van Bokhoven, J. A. *Phys. Chem. Chem. Phys.* **2015**, *17*, 3326−3331.
(43) Bhattacharjee, S.; Chen, C.; Ahn, W.-S. *RSC Adv.* **2014**, *4*, 52500−52525.
(44) Férey, G.; Mellot-Draznieks, C.; Serre, C.; Millange, F.; Dutour, J.; Surblé, S.; Margiolaki, I. *Science* **2005**, *309*, 2040−2042.
(45) Hodson, E.; Simpson, S. J. *Polyhedron* **2004**, *23*, 2695−2707.
(46) Serron, S. A.; Nolan, S. P. *Organometallics* **1995**, *14*, 4611−4616.
(47) Morris, D. J.; Clarkson, G. J.; Wills, M. *Organometallics* **2009**, *28*, 4133−4140.
(48) Gazsi, A.; Bánsági, T.; Solymosi, F. *J. Phys. Chem. C* **2011**, *115*, 15459−15466.
(49) Egerton, R. F.; Li, P.; Malac, M. *Micron* **2004**, *35*, 399−409.
(50) Sponholz, P.; Mellmann, D.; Junge, H.; Beller, M. *ChemSusChem* **2013**, *6*, 1172−1176.
(51) Serra-Crespo, P.; Ramos-Fernandez, E. V.; Gascon, J.; Kapteijn, F. *Chem. Mater.* **2011**, *23*, 2565−2572.

DOI: 10.1021/acscatal.5b01987
ACS Catal. 2015, 5, 7099−7103